Check for updates

Simultaneous amorphous silica and phosphorus recovery from rice husk poultry litter ash†

Laura Fiameni, [ID][a] Ahmad Assi, [ID][a] Ario Fahimi, [ID][a] Bruno Valentim, [ID][b] Karen Moreira,[b] Georgeta Predeanu, [ID][c] Valerica Slăvescu,[c] Bogdan Ş. Vasile, [ID][d] Adrian I. Nicoară,[d] Laura Borgese, [ID][a] Gaia Boniardi, [ID][e] Andrea Turolla, [ID][e] Roberto Canziani [ID][e] and Elza Bontempi [ID]*[a]

The livestock sector is one of the most important sectors of the agricultural economy due to an increase in the demand for animal protein. This increase generates serious waste disposal concerns and has negative environmental consequences. Furthermore, the food production chain needs phosphorus (P), which is listed as a critical raw material due to its high demand and limited availability in Europe. Manure contains large amounts of P and other elements that may be recycled, in the frame of circular economy and "zero waste" principles, and reused as a by-product for fertilizer production and other applications. This paper focuses on the extraction and recovery of amorphous silica from rice husk poultry litter ash. Two different extraction procedures are proposed and compared, and the obtained silica is characterized. This work shows that amorphous silica can be recovered as an almost pure material rendering the residual ash free of P. It also addresses the possibility of more specific phosphorous extraction procedures *via* acid leaching.

1. Introduction

Biomass waste is gaining support as a possible alternative energy source. In the Circular Economy Action Plan adopted on 11 March 2020,[1] the European Union (EU) Commission promotes access to alternative feedstock sources such as sustainable biomass. The aim is to reduce Greenhouse Gas (GHG) emissions and landfilled wastes such as animal manure. In the future, biomass will play an important role in renewable and sustainable energy development. However, the increase in biomass consumption must correspond with suitable possibilities to recover waste deriving from them.

In the last few decades, several recycled materials from livestock farming were considered and proposed for reuse, mainly as fertilizers.[2] In particular, the reuse of poultry litter (PL) shows several advantages since (a) compared to other by-products, it has a high nitrogen and phosphorus (P) content, (b) compared to other wastes it is relatively dry and consequently more adequate for energy recovery and (c) it is easier to transport.[3]

Different treatments are proposed to reuse PL, starting from composting and anaerobic digestion to direct combustion.[4] A recently published paper[3] shows that (among the proposed management strategies) Life Cycle Assessment (LCA) demonstrates that the thermal conversion of PL is the most environmentally friendly method and has a low environmental impact. Thermal treatment also has the advantage to destroy pathogen agents and organic pollutants that may be present in PL.

The waste from thermal treatments, poultry litter ash (PLA), is rich in P[5] and has a high recycling potential.[6] This makes PLA extremely interesting as a source for P recovery. Indeed, PLA has been proposed by various researchers as an alternative phosphorous source.[7–9]

P used in fertilizers and animal feed is currently obtained from phosphate rocks, which are finite and located in only a few places on Earth.[10] Therefore, the recovery and recycling of this critical raw material should be taken into consideration to have sustainable management of P. The main P-rich waste streams are sewage sludge, animal manure, slaughterhouse waste (*e.g.* meat and bone meal), and food waste. The mentioned waste materials are well described in Ohtake and Tsuneda (2019)[11] and presents the latest research advances, innovations, and applications of P recovery and recycling.

[a]INSTM and Chemistry for Technologies Laboratory, Department of Mechanical and Industrial Engineering, University of Brescia, Via Branze, 38, 25123, Brescia, Italy. E-mail: elza.bontempi@unibs.it

[b]Instituto de Ciências da Terra (ICT), Faculdade de Ciências da Universidade do Porto, Rua do Campo Alegre 1021, 4169-007 Porto, Portugal

[c]University POLITEHNICA of Bucharest, Research Center for Environmental Protection and Eco-Friendly Technologies (CPMTE), 1 Polizu St. 011061, Sector 1, Bucharest, Romania

[d]University POLITEHNICA of Bucharest, National Research Center for Micro and Nanomaterials, 6 Iuliu Maniu Bdv. 061344, Sector 6, Bucharest, Romania

[e]Politecnico di Milano, Department of Civil and Environmental Engineering (DICA) – Environmental Section, Piazza Leonardo da Vinci, 32, 20133, Milano, Italy

† Electronic supplementary information (ESI) available. See DOI: 10.1039/d0ra10120f

It is also important to highlight that the depletion of natural resources requires the continuous improvement of recovery strategies, with an emphasis on the recovery of all the waste components, even if derived from incineration processes.[12]

In particular, very recently a new idea to maximize the benefits of recovery was developed in terms of Azure Chemistry.[13] The aim was not only to replace critical raw materials (such as P) with valorised wastes (*i.e.* secondary materials) but also with the ambition of simultaneously recovering and recycling the waste derived from the critical raw material extraction to subsequently be used in other applications.[14,15] In this context, creative approaches are mandatory as a driving force not only to find suitable and sustainable ways to proceed in the recovery of critical raw materials but also to propose new and high-value applications for the recovered materials[16] that are defined eco-materials.

Eco-materials enhance environmental improvement and respect the sustainability pillars while maintaining accountable performances.[17–21]

This work can be classified as a study that addresses possible ways to manage and enhance specific biomass ash, namely rice husk poultry litter ash (RHPLA). As we have previously studied, this waste is mainly composed of K, P, Ca, S, and Si, where the amount of amorphous component is higher than 60%.[15] Obviously, in such a complex waste, containing several phases and different elements (also in low quantities), it is hard to define the exact amorphous composition. But we highlight that literature reports that the combustion of rice husk (RH), a constituent of RHPLA, produces essentially amorphous silica.[22] Silica recovered from RH has gained attention over the years due to its various applications and the virtuous example of the circular economy that it represents. Fillers, additives, desiccants, adsorbents, catalysts, mesoporous materials, nanocomposites, ceramics, biomedical sector, and heavy metal stabilization of incineration waste, are some of the fields in which value-added silica from RH could found an application.[23–27]

On this basis, the objective of this work is to propose an eco-material extraction (amorphous silica), starting from RHPLA, that can be made in combination with P recovery. RHPLA, and more in general PLA, is a type of waste that obtained visibility for reuse in a very recent period, and for this reason, literature and studies are minimal, especially about characterisation and recovery. Table 1

shows the P and Si content in different biomass ash reported in the literature. To the best of authors' knowledge, this is the first paper that presents the opportunity of a combined recovery strategy of amorphous silica and P for RHPLA.

2. Experimental

2.1. Materials and methods

2.1.1. Sampling. RHPLA was sampled at "Campoaves, S.A." (Figueira da Foz, Portugal) from an incineration plant designed for the combustion of PL. The combustion unit consists of a chain grate stoker with an over-fire airflow which regulates the temperature for combustion at $\sim$1000 °C (the temperature mostly depends on the amount of moisture in the environment). The fuel is composed of rice husk poultry litter (the rice husk is provided from rice fields which are located in the surrounding area close to the plant) and wood chips on a 70 : 30 ratio. The generated ash consists of bottom ash (BA) (that accumulates on the grate, falls into the BA wet tank and is deposited in an open-air storage area close to the plant), economizer fly ash (ECO), and fly ash captured by a multicyclone system (MCYC).

The conditions of the boiler are variable and change from month to month. On average, the plant generates 156 tons of ash per month. The quantity of ash sampled correlates with the specific conditions implemented on the sampling day. After 5 h, the samples were collected in thick plastic bags. Approximately 327 kg of BA was collected at the water tank exit, 5 kg of ECO was collected from a duct connected to the economizer with an exit point adjoining the pit where the BA sample was collected, and 10 kg of MCYC was collected from the multicyclone hopper.

The samples were dried for 24 h in aluminium trays inside an oven operating at 50 °C (as described by Fahimi *et al.* (2020)[15] and Andò (2020)[32]). After drying, the samples were manually divided into representative fractions through the coning method and then further divided into representative 100 g sub-samples using a riffle splitter.

The ashes were then sent to Chemistry for Technologies Laboratory (Univ. of Brescia), where they were grounded, and finally sieved to obtain four different fractions: <300 µm, 300–500 µm, 500–1400 µm, >1400 µm. The sieving was manually carried out with a set of ASTM International standard sieves: 50 mesh (300 µm), 35 mesh (500 µm), and 14 mesh (1400 µm).

Table 1 Phosphorus (P_2O_5) and silicon (SiO_2) content in biomass ash. * Mean value, ** data converted with conversion factors $P/P_2O_5 = 0.436$, $Si/SiO_2 = 0.468$

Biomass ash	P_2O_5%		SiO_2%		Ref.
	Fly ash	Bottom ash	Fly ash	Bottom ash	
Poultry litter ash	16.17*, **	11.47**	7.37*, **	19.66**	28
	—	12.16**	—	—	29
	—	22.00*, **	—	—	5
	—	19.38**	—	—	9
	22.71	—	3.19	—	30
Animal by-products (meat bone meal ash)	22.45**	25.96*, **	—	—	5
	32.50	—	1.80	—	30
Pig manure ash	—	22.80*	—	13.30*	30
Wood ash	0.69 **	3.21 **	7.69 **	12.39 **	31

2.1.2. Characterisation techniques

X-ray diffraction (XRD) analysis. For the structural characterisation of the raw ashes and the amorphous silica fraction obtained from the raw ashes, X-ray diffraction (XRD) analysis was conducted. XRD measurements were performed by a PANalytical X'Pert PRO diffractometer (PANalytical, Malvern, UK), equipped with a Cu Kα anode and operating at a voltage of 40 kV and a current of 40 mA. For the phase identification, Philips X'Pert software was used (associated with the crystallography open database (COD)) as described by Assi *et al.* (2019).[33]

Scanning electron microscopy combined with energy-dispersive X-ray spectrometry (SEM-EDXS). Morphological and dimensional characterization of the ash and silica powder samples were performed through scanning electron microscopy (SEM) (LEO EVO 40, Carl Zeiss AG, Milan, Italy), coupled with an EDXS (energy dispersive X-ray spectroscopy, Oxford instruments, Wiesbaden, Germany) probe for elemental analysis and semi-quantitative chemical characterization. The material topography was analysed using the secondary electron (SE) mode.

Total reflection X-ray fluorescence (TXRF) analysis. The TXRF technique was used for elemental analysis in a solution. A stock solution of 1 g L-1 Ga in nitric acid (Ga-inductively coupled plasma (ICP) Standard Solution, Fluka, Sigma Aldrich) was used as the internal standard. Approximately 0.010 g of 100 mg L^{-1} of Ga solution prepared from the stock solution was added to the samples and properly diluted with MQ water to obtain a final concentration of 1 mg L^{-1} Ga in 1 mL specimens. The specimens were then homogenized using a vortex shaker for 1 min at 2500 rpm.[19] For each specimen of the digested and leachate solution, a 10 μL drop was deposited on three different plexiglass reflectors and dried on a hot plate at 50 °C under a laminar hood. Each reflector was irradiated for 600 s of live time using an S2 Picofox system (Bruker AXS Microanalysis GmbH, Berlin, Germany) equipped with a Mo tube (operating at 50 kV and 750 mA) and a silicon drift detector (SDD). An instrumental software with a routine deconvolution based on mono-element profiles was applied to evaluate the peak areas and analyse the TXRF spectra. Since lighter elements such as P and S can be underestimated by the TXRF analysis under the reported experimental conditions,[34] a dedicated calibration curve was developed for S and P to correct for matrix effects following the approach reported by Borgese *et al.* (2018).[35]

Element concentrations present in the acid leaching solution were converted into extracted mass using the formula:

$$\text{Extracted mass (mg kg}^{-1}) = (C \times \text{DF} \times V) \times m^{-1}$$

in which: C = concentration of the analyte by TXRF analysis (mg L^{-1}); DF = dilution factor; V = volume of extractant (mL); m = mass of ash weighed for leaching (g)

X-ray fluorescence (XRF) analysis. For qualitative and quantitative analysis of the elements, an X-ray Sequential Fluorescence Spectrometer Thermo Scientific ARL PERFORM'X equipped with an X-ray tube with Rh anode and Be window of 30 μm was used. The entire surface of the sample was analysed in a dry He flow.

Phosphorus quantification via UV-Vis chemical method. The method was developed following the Romanian standardized method.[36] RHPLA raw samples were prepared at a grain size of less than 0.2 mm and the amount was 0.1 g with a 0.0001 g measured accuracy. Then, RHPLA samples were solubilized with a mixture of concentrated acids 2 : 1/H_2SO_4 : HNO_3. To prevent the colorimetry operation, the silicic acid that produces the opaque solution was removed by filtration. The analysis was carried out by adding ammonium molybdate and H_2SO_4 6 N solutions. The P concentration in the filtrate was encapsulated in phosphomolybdate $[(NH_4)_6Mo_7O_{24}\cdot 4H_2O]$ and the absorbance of the resulting blue solution was measured at 700 nm wavelength by a suitable optical instrument. The measurements were done in 2 cm thick cuvettes. As a reference, a blank solution of the reagents, without the ash, passed through all the analytical steps was used. The spectrophotometer was set to perform three readings and the average was taken. On the calibration curve with a 0.993 regression coefficient, the P content corresponding to the extinction obtained on the spectrophotometer was read.

The preparation of the reagents was carried out just before the analysis, performed with a JASCO V570 UV-VIS spectrophotometer at UPB - CPMTE laboratory.

The P content in ash was calculated using the formula:

$$\% \text{ Phosphorus (P)} = e \times m^{-1} \times 100$$

in which: e = P content, mg (read on the calibration curve). m = mass of the ash sample in the 50 mL colorimetric solution, mg.

2.2. Silica and phosphorus recovery

2.2.1. Procedure A.
Procedure A was conducted using the method proposed by Bosio *et al.* (2014)[37] and Kamath *et al.* (1998).[38] 50 g of each ash sample was placed in a beaker and 416 mL of 1 mol L^{-1} NaOH solution was added. Constant stirring was maintained at 100 °C for 1 h. The solutions from samples ECO and MCYC containing sodium silicate [reaction 1], still warm, were filtered under slight suction through Whatman filter paper grade 589/2 white ribbon filter ashless (pore size 4–12 μm). However, the filtration of the BA sample was slow and difficult, and it was first filtered through a Whatman filter paper grade 589/1 black ribbon ashless (pore size 12–25 μm) before passing to the finer porosity. Sedimentation, which led to phase separation, was useful for better percolation. The BA sample leachate was clear but dark brown in colour, while the other solutions were clear and colourless.

$$\text{SiO}_{2(s)} + 2\,\text{NaOH}_{(aq)} \rightarrow \text{Na}_2\text{SiO}_{3(aq)} + \text{H}_2\text{O}_{(l)} \quad \text{(reaction 1)}$$

After filtration, 60 mL of 1 mol L^{-1} H_2SO_4 solution was slowly added, at room temperature and constant stirring, to each 200 mL of leachate. Chemical conditions of the reaction govern the kinetic, the mechanism of hydrolysis, and the condensation processes.[39] Therefore, the gel formation was controlled by pH measurement to reach the best endpoint of the gelling reaction. The acid solution was further added dropwise until a pH of 9.8 was reached, and then the titration was stopped. A volume

ranging between 20 and 40 mL, depending on the ash leachate, was added after the first H_2SO_4 addition. The formation of silica gel from the sodium silicate solution was performed in accordance with [reaction 2].

$$Na_2SiO_{3(aq)} + H_2SO_{4(aq)} \rightarrow SiO_{2(gel)}$$
$$+ Na_2SO_{4(aq)} + H_2O_{(l)} \qquad \text{(reaction 2)}$$
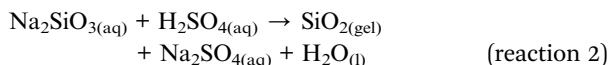
After 7 days of aging, the gels were completely formed, however, they were still mixed with reaction water. A centrifuge (Eppendorf, Centrifuge 5804 R) was used to separate the gel from the solution. The mixture was transferred to a 50 mL centrifuge tube and centrifuged at 1000 rcf for 10 min at 20 °C. The supernatant was separated and stored in a polyethylene tube, while the gel was dried with an electric oven at 120 °C for 7–10 h (halogen convection furnace Bonny 2172339, Kooper, Rome, Italy). The final BA silica gel was brown, while the other two gels were whitish, even after drying. For subsequent XRD analysis, the gels were grounded using a mixer mill MM 400 (Retsch, Haan, Germany).

2.2.2. Procedure B. The second procedure is based on work from Santana Costa *et al.* (2018).[40] 30 g of each ash was placed in a beaker with a 1 mol L^{-1} HCl solution at a solid/liquid (S/L) ratio of 1 : 10 and constantly stirred at room temperature for 2 h. After this period, the acid leachates of ECO and MCYC were filtered under slight suction through Whatman filter paper grade 589/2 (pore size 4–12 μm) and stored in polyethylene tubes for further TXRF analysis. The solid residues were washed with MQ water until a constant pH was reached, dried, and then the washed water was stored separately in polyethylene tubes. It was not possible to filter the BA acid suspension due to its fine porosity and the sample was instead centrifuged at 20 °C for 20 min at 1000 rcf with a 50 mL centrifuge tube (Eppendorf, Centrifuge 5804 R). The supernatant was separated and stored in a polyethylene tube for further TXRF analysis. The solid residue was washed with MQ water until a constant pH was reached, dried, and then, by using the procedure described previously, separated from the wash waters and stored in polyethylene tubes.

All the solid samples after acid pre-treatment were dried in an electric oven at 120 °C for 9 h (halogen convection furnace Bonny 2172339, Kooper, Rome, Italy). A weight loss of 64.1% for BA and ECO and 72.8% for MCYC was recorded.

To conform with [reaction 1], these samples were reacted with a 4 mol L^{-1} NaOH solution, in an S/L ratio 1 : 10, under constant stirring at 80 °C for 4 h. At the end of the reaction, the mix was allowed to cool and settle at room temperature for 24 h.

The separation of sodium silicate solutions from the solid residues was performed under slight suction through Whatman filter paper grade 589/2 and 589/1 (pore size 4–12 μm and 12–25 μm). The solid residues were then washed with MQ water until a constant pH was reached, dried with an electric oven (halogen convection furnace Bonny 2172339, Kooper, Rome, Italy), and stored in plastic bags. The washing waters were stored in polyethylene tubes. During the procedure, a volume loss for the

sodium silicate solutions was recorded: 25% for ECO and MCYC and 40% for BA.

To comply with [reaction 2], a 5 mol L^{-1} H_2SO_4 solution was added dropwise to each 50 mL of sodium silicate solution, under constant stirring at room temperature, in order to lower the pH to 9.8 and to form the gel. After the period of aging, the silica gel separation from the reaction water was carried out in the same way as described in procedure A. A Neya centrifuge model 16-R was used, operated at 5000 rpm for 20 min at 25 °C. Subsequent drying in the oven lasted 5–6 h. The BA silica gel was brown, while the ECO and MCYC gels were whitish. For subsequent XRD analysis, the gels were ground with a mixer mill MM 400 (Retsch, Haan, Germany).

3. Results and discussion

3.1. Rice husk poultry litter ash (RHPLA) characterisation

Fig. 1 shows the XRD patterns of the raw RHPLA (BA, ECO, and MCYC) samples compared to the same samples after the acid pre-treatment step of procedure B. As shown in Fig. 1A (spectrum BA-A), BA contains quartz [SiO_2], sylvite [KCl], and arcanite [K_2SO_4] as identified by the main peaks at 26.62°, 28.31° and 30.77° in 2θ (2 theta) respectively. All the other crystalline phases are phosphate compounds of Na, Ca, K, and Mg namely sodium hydrogen phosphate [NaH_2PO_4], sodium-calcium phosphate [$Na_2CaP_2O_7$], calcium phosphate [$Ca_3(PO4)_2$], sodium hydrogen phosphate hydrate [$Na_3HP_2O_7(H_2O)$], and potassium magnesium orthophosphate hydrate [$KMgPO_4(6H_2O)$].

The presence of a broad band in all the XRD patterns BA-B (Fig. 1A), ECO-B (Fig. 1B), and MCYC-B (Fig. 1C) between 15 and 35° in 2θ, demonstrates that an amorphous phase is also present in these samples.[38]

The broad X-ray diffraction halo in the XRD pattern is typical for amorphous compounds.[41] Consequently, even if this type of bottom ash (BA) was characterized for the first time by the XRD technique in this paper, the presence of an amorphous phase can be assumed seeing as it has already been reported for fly ash with the same origin by Fahimi *et al.* (2020).[15] This amorphous component in all the samples may consist of both silicon oxide, widely found and studied for ash originating from rice husk combustion,[42–44] and P phases, as confirmed by the Raman and XRD analyses in ECO and MCYC samples made by Fahimi *et al.* (2020)[15] also per Stammeier *et al.* (2018).[45] The spectrum BA-B in Fig. 1A shows that after the acid leaching, the initial complex matrix loses its soluble components, maintaining only two crystalline phases: quartz [SiO_2] and sylvite [KCl]. The compound KCl is present in a different crystalline phase from the raw BA sample seeing as it shows the main peak at 34.88° in 2θ which was previously absent. Also, the differences between the crystalline phases in BA-A and BA-B (Fig. 1A) suggest that phosphate soluble compounds are leached by HCl. The same can be assumed for the ECO and MCYC samples.

Spectrum ECO-A (Fig. 1B) and spectrum MCYC-A (Fig. 1C) show that ECO and MCYC, similar to BA, contain quartz [SiO_2], sylvite [KCl], and potassium sulphate (or arcanite) [K_2SO_4] as identified by the same main peaks found in BA-A (26.6°, 28.3° and 30.8° in 2θ). All the raw samples contain the same crystalline phosphate phase: sodium hydrogen phosphate [NaH_2PO_4]. Sodium calcium
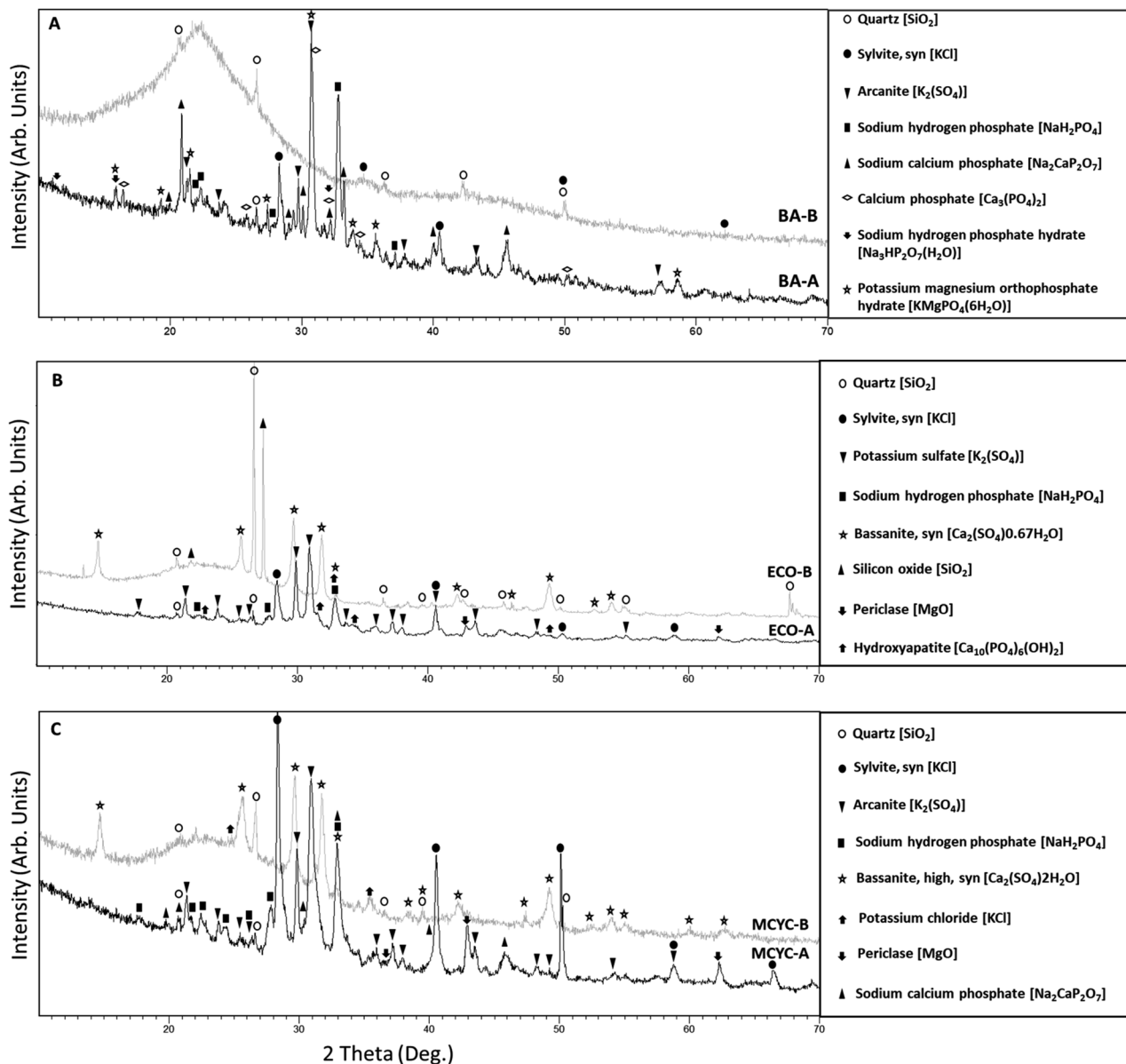
Fig. 1 XRD patterns obtained for the samples BA (A), ECO (B) and MCYC (C): raw RHPLA in black (BA-A, ECO. A, MCYC-A) and raw RHPLA after the acid leaching with HCl 1 mol L^{-1} for procedure B in grey (BA-B, ECO-B, MCYC-B).

phosphate [Na$_2$CaP$_2$O$_7$] was observed in MCYC as well as in the BA sample, while hydroxyapatite [Ca$_{10}$(PO$_4$)$_6$(OH)$_2$] was found only in ECO (Fig. 1B ECO-A). Hydroxyapatite and sylvite were previously found in similar wastes[46] and some of the detected crystalline phases are those previously found by Fahimi *et al.* (2020).[15] Lastly, Periclase [MgO] was found in both fly ash samples (spectra ECO-A and MCYC-A in Fig. 1B and C). After the acid pre-treatment, spectra ECO-B and MCYC-B (Fig. 1B and C) show the presence of an amorphous phase and remaining crystalline phases quartz/silicon oxide [SiO$_2$] and bassanite [Ca$_2$(SO$_4$)yH$_2$O]. A residual amount of potassium chloride [KCl] was detected for MCYC-B (Fig. 1C) in a phase very similar to that found in BA-B (Fig. 1A). Similar to BA, after the acid treatment, phosphatic compounds are absent in ECO and MCYC.

The crystalline phase identification is corresponding to the XRF data reported in Table 2 for each raw RHPLA and its corresponding ash after acid leaching with procedure B.

The raw ashes formed from the combustion of three main fuels: rice husk, poultry droppings, and wood chips that have high concentrations of silicon (SiO$_2$), phosphorus (P$_2$O$_5$), and calcium (CaO) respectively. However, as shown in Table 2, the main constituent of these samples is potassium (K$_2$O). Additionally, SO$_3$, MgO, Na$_2$O, and Cl are present in lower concentrations. Other metals, such as Al$_2$O$_3$, MnO, Fe$_2$O$_3$, NiO, CuO, and ZnO are present in negligible amounts. These results confirm the importance of recovering both P and silicon (Si) from this waste typology.

XRF analysis of ash samples after acid pre-treatment reported in Table 2, also corroborates the previous hypothesis that P-compounds are leached by HCl, while Si remains in the

Table 2 XRF chemical composition of raw RHPLA and raw RHPLA after acid leaching with HCl 1 mol L^{-1} in procedure B. nd: not detected. Others contains: TiO_2, Cr_2O_3, Rb_2O, BaO, SrO, Br, V_2O_5 and SeO_2

|	BA		ECO		MCYC	
	Raw RHPLA	Leaching HCl 1 mol L^{-1}	Raw RHPLA	Leaching HCl 1 mol L^{-1}	Raw RHPLA	Leaching HCl 1 mol L^{-1}
Compositions	Results in wt%					
Na_2O	2.91	nd	2.88	nd	2.95	nd
MgO	5.83	1.01	3.90	0.49	6.15	0.94
Al_2O_3	0.84	1.03	0.43	0.66	0.64	4.50
SiO_2	10.26	56.67	12.76	47.96	9.86	32.04
P_2O_5	18.89	6.60	12.67	3.58	17.62	21.41
SO_3	7.23	14.82	17.20	27.52	13.82	17.10
Cl	1.34	6.89	2.42	1.52	3.52	0.45
K_2O	30.72	4.10	33.10	1.33	28.28	3.85
CaO	18.60	3.52	12.02	13.17	14.13	13.34
MnO	0.58	0.21	0.36	0.10	0.48	0.32
Fe_2O_3	1.19	2.83	0.64	1.95	0.97	3.93
NiO	0.01	0.02	0.01	0.01	0.01	0.01
CuO	0.11	0.49	0.07	0.26	0.08	0.24
ZnO	0.30	0.25	0.43	0.13	0.36	0.42
Others	0.17	0.53	0.09	0.27	0.11	0.38

matrix and is purified for subsequent recovery. As shown in Table 2, during the leaching process, BA lost P_2O_5, K_2O, and CaO, while maintaining SiO_2, SO_3, and Cl. In ECO evident leaching of K_2O, P_2O_5, and other minor components occurred. However, SiO_2, SO_3, and CaO remain in high percentages in the sample. For MCYC, the P-leaching was not so effective, and the amounts of P_2O_5, SiO_2, and SO_3 in the RHPLA residues remain quite high (P_2O_5 at 21.41%). The leaching of K_2O occurred. According to the results expressed as w/w% it can be observed that the major content of SiO_2 after the acid pre-treatment is detected in BA. After acid leaching with HCl 1 mol L^{-1} as described in procedure B, BA seems more purified compared to ECO and MCYC because most of the components are contained in minor concentrations. However, the BA complex matrix, rich in organic matter and hydrocarbon compounds, is not the best starting material for silica recovery, due to its composition and dark colour, as seen during the experimental.

The quantification of P by XRF and chemical method is reported (for comparison) in Fig. 2. Also, Fig. S.1 (ESI†) reports the description of the UV-Vis method that was adapted for phosphorous quantification:[36] it was considered suitable for RHPLA since it is a material with high P content and the method is based on colorimetric tests to obtain the extinction values on the calibration curve. XRF results reveal, in the three raw RHPLA, a P content between 4.9 and 7.1%, while UV-Vis data between 3.9 and 7.9%.

In Fig. 3 an image for each RHPLA sample (scale bar 2 mm), BA (A), ECO (B), MCYC (C), is provided. For points P.1 (Fig. 3B) and P.2 (Fig. 3C) respectively located in the ECO and MCYC samples, a higher magnification analysis was carried out as reported in Fig. 3D and E. The chemical composition measured with EDXS of points P.1, P.2, P.3, P.4 is shown in the spectra below. Phosphospheres were identified in ECO (Fig. 3B P.1) and MCYC (Fig. 3C P.2) and are distinguishable due to their (spherical) shape and semi-smooth surface which was covered

with micrometric particles of other elements. Although the phosphosphere shown in Fig. 3E is very "clean" compared to the phosphosphere in Fig. 3D, their respective compositions reported in spectra P.1 and P.2 are relatively similar.

The main constituent element for these two points, besides O and K, is P. Other spheres like these were detected during the analysis and, as can be seen from Fig. 3, their dimensions vary from less than 100 to 300 μm. Similar to findings made by Fahimi et al. (2020),[15] the two fly ash samples (ECO and MCYC) consist of micrometric and supermicrometric (<10 μm and >10 μm respectively) P-rich morphotypes. Valentim et al. (2016)[47] reported that Si-, Ca-, K- and Mg-phosphospheres (P-rich glassy spheres) are a type of amorphous material that can frequently be observed in biomass fly ash. Points P.3 and P.4 (Fig. 3D and spectra P.3 and P.4) show high concentrations of Si and O, and their surfaces are covered mainly with K but also with Na, Mg, P, S, Cl, and Ca. The presence of an amorphous P-phase (P.1 and P.2) and an amorphous Si-phase (P.3 and P.4) are reconfirmed by the SEM-EDXS analysis.
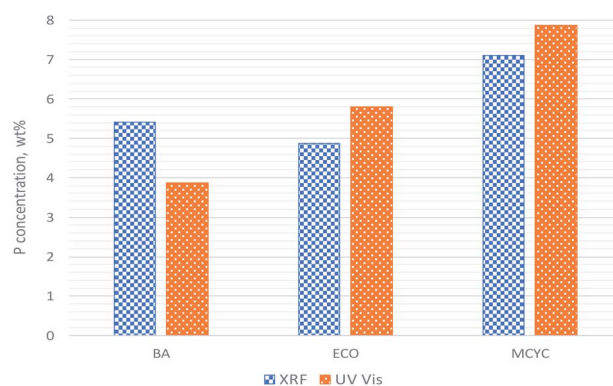

Fig. 2 Comparison of XRF and UV-Vis results for P quantification in raw RHPLA.

3.2. Silica characterisation

As previously mentioned, the XRF analysis in Table 2 shows a significant reduction or total leaching of P_2O_5 and alkali metals, while SiO_2 remains in the matrix. The acid pre-treatment of procedure B therefore allows the lowering of salt contents in the final dried silica, as shown by the XRD analysis in Fig. 4. Fig. 4A shows that, for silica recovered with procedure A, thernadite and sodium sulphate $[Na_2SO_4]$ with potassium sodium sulphate phases were identified. It should be noted that there are several crystalline phases for procedure A, while for procedure B (Fig. 4B), the final product is contaminated only by thernadite and sodium sulphate with the same chemical
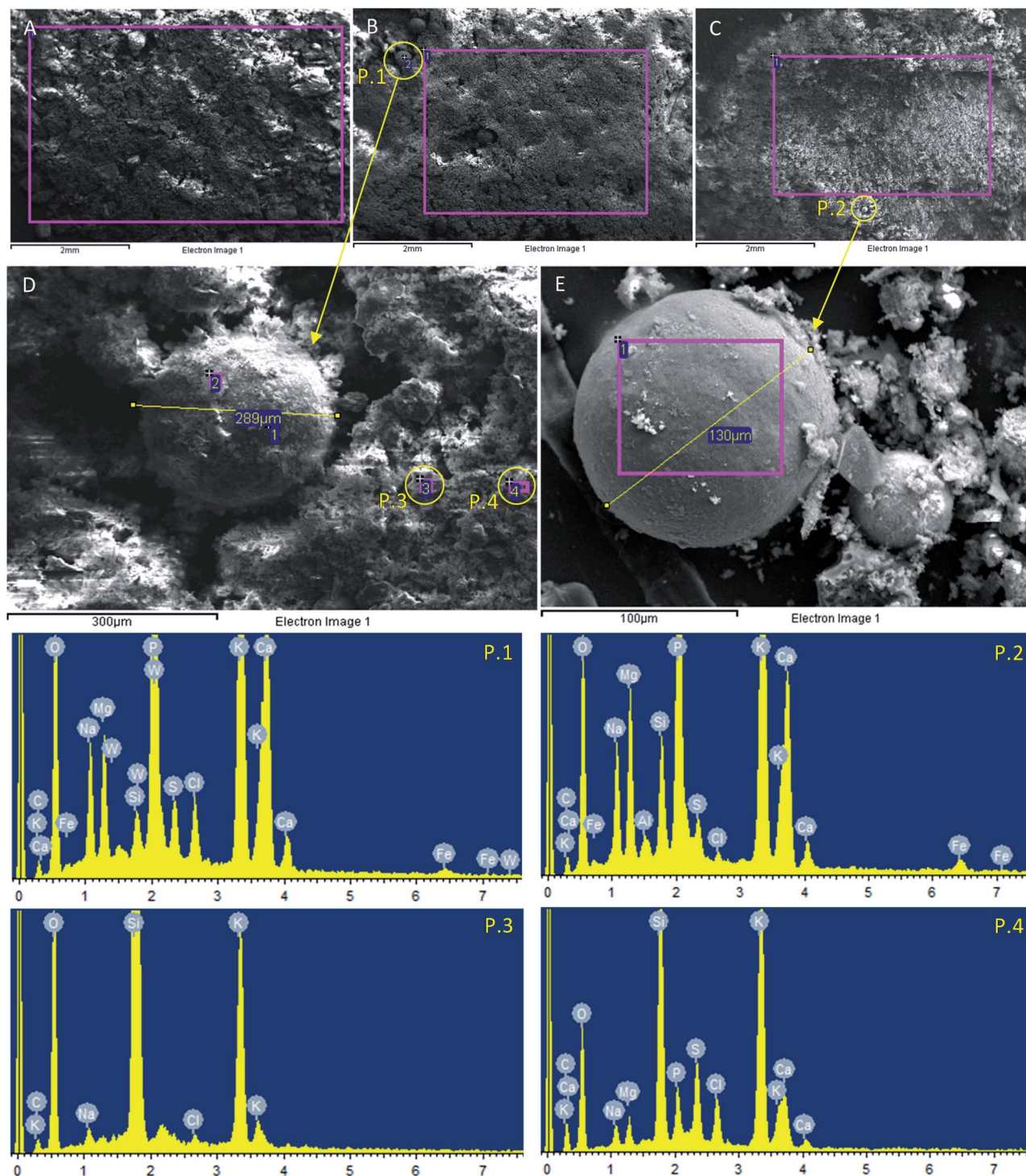
Fig. 3 SEM images of raw RHPLA: BA (A), ECO (B), MCYC (C) with a length of ~2 mm. Micrometric spherical morphotypes marked with P.1 and P.2 and their magnification shown in (D) and (E). EDXS chemical composition of the points P.1, P.2, P.3 and P.4 in the spectra below.
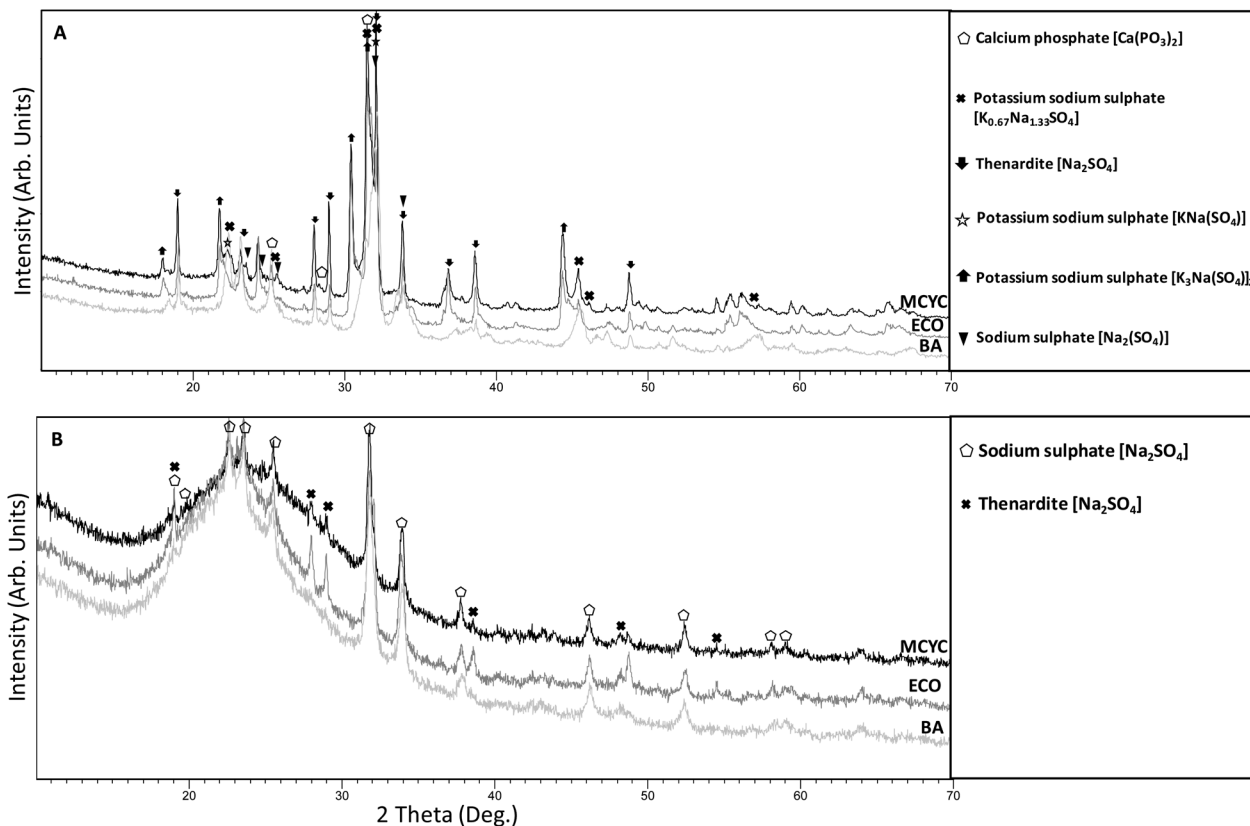
Fig. 4 XRD patterns of silica obtained from procedure A (A) and from procedure B (B): silica BA in grey, silica ECO in dark grey, silica MCYC in black.

formula [Na_2SO_4]. The presence of these compounds is justified by [reaction 2] where Na_2SO_4 is a reaction product together with SiO_2. During the aging of the gel, a certain amount of Na_2SO_4, soluble in the reaction solution, may be trapped in the hygroscopic silica network, and then recrystallized during drying.

Moreover, from the XRD analysis of recovered silica from procedure B (Fig. 4B), an amorphous phase is identified from the broad halo present in all the XRD patterns from about 15 to 35° in 2 theta. These assessments suggest that procedure B was more effective and data in Table 3 validate this hypothesis. XRF analysis of the six samples of recovered amorphous silica, results provided in Table 3, indicates that the SiO_2 content in the gels from procedure A was very low compared to procedure B. Na_2O, SO_3 and K_2O contaminate amorphous silica A much more than the amorphous silica B. The absence of an acid pre-treatment in procedure A leads to P_2O_5 still being present in the final amorphous recovered product, wasting P and contaminating the silica. On the other hand, SiO_2, Na_2O, and SO_3 are the significant components in amorphous silica B, and the only crystalline phase detected by XRD, namely thernadite/sodium sulphate [Na_2SO_4] (Fig. 4B), justifies the presence of sodium and sulphur in the XRF analysis of these samples. As reported in Table 3, ECO B has the highest silica content at 80.30%. Nevertheless, all the samples produced with procedure B show higher values of SiO_2% due to the low presence of crystalline phases compared to the silica from procedure A that contains

a lot of salts. This means that procedure B allows the obtainment of an almost pure final product in three steps: acid leaching pre-treatment, [reaction 1], and [reaction 2].

3.3. Acid leachate characterisation

In procedure B for silica extraction, a pre-treatment with 1 mol L^{-1} HCl solution was used, as proposed by Alvarez *et al.* (2015),[48] to obtain better results in terms of purity of the extracted silica. As is well known for other different starting materials, such as sewage sludge ash (SSA), the most common method for P-recovery is acid leaching.[49–51] The choice to use HCl as an extractant in this work was done in accord with the reference article on which the procedure B was based,[40] following literature about SSA: Hong *et al.* (2005),[52] Biswas *et al.* (2009),[53] Xu *et al.* (2012),[54] Petzet *et al.* (2012)[55] and the recent Semerci *et al.* (2020),[56] that demonstrates the effective recovery of P with HCl.

A recent paper[57] shows that wet chemical leaching approaches appear to be the most sustainable method for P extraction from SSA and the current research proceeds in this direction.

The main advantage of the proposed method is that the RHPLA contains low quantities of heavy metals compared to SSA. In particular, great attention to fertilizer regulations (the first area of interest for the application of recovered P) must be given regarding maximum concentrations of As, Cd, Hg, Cr(vi),

Table 3 XRF chemical composition of recovered amorphous silica using procedure A and B. nd: not detected. Others contains: Fe_2O_3, ZnO, CuO, MnO and BaO

Compositions	Procedure A			Procedure B		
	Silica BA	Silica ECO	Silica MCYC	Silica BA	Silica ECO	Silica MCYC
	Results in wt%					
SiO_2	23.38	14.98	21.70	77.48	80.30	73.11
Na_2O	22.99	19.39	16.89	9.29	8.68	9.30
SO_3	35.35	39.08	35.17	10.67	9.32	5.78
P_2O_5	3.68	2.93	4.61	0.09	0.08	0.30
K_2O	11.08	20.53	17.65	0.12	0.08	1.05
Cl	0.71	1.43	2.31	0.08	0.04	0.02
CaO	0.59	0.01	0.01	0.09	0.03	0.02
MgO	0.54	0.45	0.40	0.13	nd	nd
Al_2O_3	0.52	0.11	0.18	0.42	0.20	8.30
Others	0.13	0.06	0.03	0.47	0.15	1.05

Ni, Cu, Pb, and Zn.[58,59] Regulation (EC) No 2003/2003 of the European Parliament and of the Council relating to fertilizers[60] will be repealed with effect from 16 July 2022 by regulation (EU) 2019/1009 laying down rules on the market availability of EU fertilizing products.[61] The limits of contaminants in fertilizers and soil improvers are reported in Table S.2 (ESI†) and compared with Fig. 5. Fig. 5 highlights the concentration of the elements of interest for the discussion, in the acid leaching solution, derived from TXRF results. The complete TXRF elemental analysis is reported in Table S.3 (ESI†). P is detected between 57 and 75 g kg^{-1}, or 5.7 and 7.5%, in the three RHPLA leachate samples. Arsenic (As), cadmium (Cd), and mercury (Hg) were not detected in the samples. Hexavalent chromium (Cr VI) is fixed at 2 mg kg^{-1}, but TXRF analysis provides an elemental analysis that cannot discriminate between elemental speciation. To set the precise value of hexavalent chromium in the samples, different analytical techniques are required. In any case, the highest concentration of total chromium is recorded for BA at about 46 mg kg^{-1}. Nickel (Ni) must respect the limit of

50 or 100 mg kg^{-1}, and in MCYC it is present at more or less 44 mg kg^{-1}. Copper (Cu) is detected in concentrations ranging between 15 and 112 mg kg^{-1}, with a limit fixed at 300 or 600 mg kg^{-1}. The same for lead (Pb), which has a limit of 120 mg kg^{-1}, and it is present in BA at more or less 5 mg kg^{-1}. Contrary, zinc (Zn) shows the following concentrations: about 0.7 g kg^{-1} for BA, about 2.5 g kg^{-1} for ECO, and about 1.9 g kg^{-1} for MCYC, while the limit is fixed at 0.8 or 1.5 g kg^{-1}. In this specific case, the limit is only respected by BA: the use of P recovered from RHPLA to prepare fertilizers or soil improvers, through the precipitation of a solid product from the RHPLA acid leachate, shall be developed to keep this contaminant within the legal limit. So, the leaching with an acid that has a high P extraction capacity, which is not preferred in literature for SSA due to metal leaching,[62,63] may be a good solution for P-recovery from RHPLA for fertilizer applications, because the main limitation is only provided by Zn concentration in the solution. The P thus extracted may undergo the same treatments already studied for SSA,[64,65] and recently proposed for poultry manure,[66] to obtain
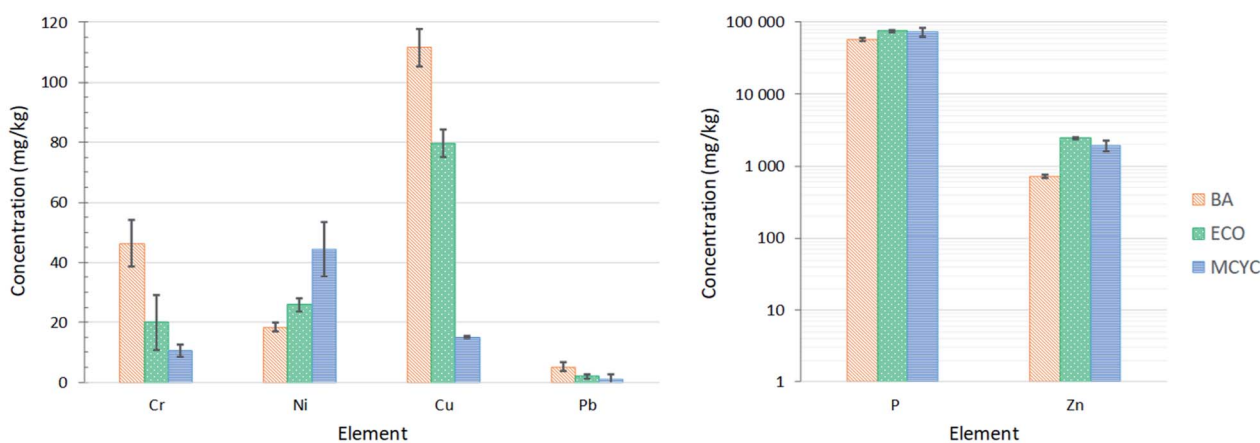
Fig. 5 TXRF analysis of acid leachate with HCl 1 mol L^{-1} for the three RHPLA under examination: BA in orange, ECO in green and MCYC in blue. Phosphorus and contaminants of interest for the preparation of fertilizers are reported. Concentration values can be compared with the limit values in Table S.2 (ESI†). Other elements concentrations for TXRF analysis are reported in Table S.3 (ESI†).

a novel product and a novel eco-material for the fertilizer industry. It is evident that the proposed procedure is suitable to promote P separation before proceeding with silica recovery and the two stages can be studied with a mutual approach as already achieved for SSA.[67,68] This first attempt of double recovery (P and SiO_2) from raw RHPLA could also present the opportunity for the reuse of RHPLA residual. The alkali leaching step with NaOH in the silica recovery procedure could leave a certain amount of Si-amorphous phase in the matrix: this may suggest a more in-depth study of extraction efficiency or a new study for further application of the RHPLA residual in Portland cement-based materials as already proposed for incinerated sewage sludge ash (ISSA).[69,70]

4. Conclusions

To the authors' knowledge, this is the first work that proposes a procedure to recover P and silica simultaneously from RHPLA.

Firstly, XRD and SEM-EDXS characterization analyses of poultry litter bottom ash (BA) were made. The results show that BA is composed of different crystalline phosphate compounds namely: sodium-calcium phosphate [$Na_2CaP_2O_7$], calcium phosphate [$Ca_3(PO4)_2$], sodium hydrogen phosphate hydrate [$Na_3HP_2O_7(H_2O)$], and potassium magnesium orthophosphate hydrate [$KMgPO_4(6H_2O)$]. In all the ash samples (BA, ECO and MCYC), together with quartz, sylvite, and arcanite, phosphate is present as sodium hydrogen phosphate [NaH_2PO_4], while Hydroxyapatite emerges only in the ECO sample. Amorphous phases of both Si and P are present in ECO and MCYC and phosphospheres were identified. The XRD analysis clearly shows these amorphous phases are purified from the soluble forms after procedure B acid leaching. EDXS analysis confirms that P, Na, Mg, S, K, and Ca are leached by the acid, while Si remains in the solid matrix. Therefore, in procedure B, Si and P were extracted separately and acid leaching was essential to obtain purified dried silica. The best result was obtained for sample ECO (about 80% SiO_2 grade). It can be concluded that procedure B can be a combined process to recover firstly P and then silica in two subsequent steps. Moreover, considering this process as a flow that produces, respectively, acid leachate containing P, RHPLA residues, and amorphous silica, we can further report that: evidence that the acid leachate contains a very small quantity of contaminants (As, Cd, Hg, Ni, and Pb) compared to the sewage sludge ash (SSA) leachate, allows the conclusion that RHPLA is a good secondary source of P that can be precipitated to obtain an eco-material candidate for industrial fertilizer production such as struvite, with particular attention to Zn concentration. RHPLA residues can be used as a binder in porous materials to improve mechanical performance or can be studied for further application in the Portland cement industry. And finally, the dried silica can be tested for the stabilization of heavy metals in Municipal Solid Waste Incinerated Fly Ash (MSWI-FA). Further studies are needed to assess whether silica may be obtained together with P from SSA.

In conclusion, optimization of procedure B can be a forthcoming activity to find the best conditions for the acid leaching and the alkali steps to obtain a good yield for both P and silica (DoE).

Author contributions

Conflicts of interest

The authors report that there are no conflicts of interest to declare.

Acknowledgements

Notes and references

1 European Commission, *Circular Economy Action Plan*, 2015. https://ec.europa.eu/environment/circular-economy/.

2 H. Kominko, K. Gorazda and Z. Wzorek, Potentiality of sewage sludge-based organo-mineral fertilizer production in Poland considering nutrient value, heavy metal content and phytotoxicity for rapeseed crops, *J. Environ. Manage.*, 2019, **248**, 109283, DOI: 10.1016/j.jenvman.2019.109283.

3 S. Nusselder, L. G. de Graaff, I. Y. R. Odegard, C. Vandecasteele and H. J. Croezen, Life cycle assessment and nutrient balance for five different treatment methods for poultry litter, *J. Cleaner Prod.*, 2020, **267**, 121862, DOI: 10.1016/j.jclepro.2020.121862.

4 B. P. Kelleher, J. J. Leahy, A. M. Henihan, T. F. O'Dwyer, D. Sutton and M. J. Leahy, Advances in poultry litter disposal technology – a review, *Bioresour. Technol.*, 2002, **83**, 27–36, DOI: 10.1007/s11668-016-0088-z.

5 L. Leng, A. A. Bogush, A. Roy and J. A. Stegemann, Characterisation of ashes from waste biomass power plants and phosphorus recovery, *Sci. Total Environ.*, 2019, **690**, 573–583, DOI: 10.1016/j.scitotenv.2019.06.312.

6 J. P. Blake and J. B. Hess, Suitability of poultry litter ash as a feed supplement for broiler chickens, *J. Appl. Poult. Res.*, 2014, **23**, 94–100, DOI: 10.3382/japr.2013-00836.

7 J. P. Blake and J. B. Hess, Poultry litter ash as a replacement for dicalcium phosphate in broiler diets, *J. Appl. Poult. Res.*, 2014, **23**, 101–107, DOI: 10.3382/japr.2013-00838.

8 D. S. Pandey, M. Kwapinska, J. J. Leahy and W. Kwapinski, Fly ash from poultry litter gasification - Can it be utilised

in agriculture systems as a fertiliser?, *Energy Procedia*, 2019, **161**, 38–46, DOI: 10.1016/j.egypro.2019.02.056.

9 K. Kaikake, T. Sekito and Y. Dote, Phosphate recovery from phosphorus-rich solution obtained from chicken manure incineration ash, *Waste Manag.*, 2009, **29**, 1084–1088, DOI: 10.1016/j.wasman.2008.09.008.

10 European Commission, *Study on the EU's list of Critical Raw Materials – Final Report*, 2020. DOI: 10.2873/11619.

11 H. Ohtake, S. Tsuneda, *Phosphorus Recovery and Recycling*. Springer, 2019. DOI: 10.1007/978-981-10-8031-9.

12 L. Benassi, A. Zanoletti, L. E. Depero and E. Bontempi, Sewage sludge ash recovery as valuable raw material for chemical stabilization of leachable heavy metals, *J. Environ. Manage.*, 2019, **245**, 464–470, DOI: 10.1016/j.jenvman.2019.05.104.

13 A. Zanoletti, F. Bilo, L. E. Depero, D. Zappa and E. Bontempi, The first sustainable material designed for air particulate matter capture: An introduction to Azure Chemistry, *J. Environ. Manage.*, 2018, **218**, 355–362, DOI: 10.1016/j.jenvman.2018.04.081.

14 M. Pasquali, A. Zanoletti, L. Benassi, S. Federici, L. E. Depero and E. Bontempi, Stabilized biomass ash as a sustainable substitute for commercial P-fertilizers, *Land Degrad. Dev.*, 2018, **29**, 2199–2207, DOI: 10.1002/ldr.2915.

15 A. Fahimi, F. Bilo, A. Assi, R. Dalipi, S. Federici, A. Guedes, *et al.*, Poultry litter ash characterisation and recovery, *Waste Manag.*, 2020, **111**, 10–21, DOI: 10.1016/j.wasman.2020.05.010.

16 F. Bilo, S. Pandini, L. Sartore, L. E. Depero, G. Gargiulo, A. Bonassi, *et al.*, A sustainable bioplastic obtained from rice straw, *J. Cleaner Prod.*, 2018, **200**, 357–368, DOI: 10.1016/j.jclepro.2018.07.252.

17 K. Halada and R. Yamamoto, The current status of research and development on ecomaterials around the world, *MRS Bull.*, 2001, **11**, 871–879.

18 A. Assi, F. Bilo, A. Zanoletti, J. Ponti, A. Valsesia, R. La Spina, *et al.*, Review of the reuse possibilities concerning ash residues from thermal process in a medium-sized urban system in Northern Italy, *Sustain*, 2020, **12**, 1–21, DOI: 10.3390/su12104193.

19 A. Assi, F. Bilo, A. Zanoletti, J. Ponti, A. Valsesia, R. La Spina, *et al.*, Zero-waste approach in municipal solid waste incineration: Reuse of bottom ash to stabilize fly ash, *J. Cleaner Prod.*, 2020, **245**, 118779, DOI: 10.1016/j.jclepro.2019.118779.

20 A. Zanoletti, F. Bilo, S. Federici, L. Borgese, L. E. Depero, J. Ponti, *et al.*, The first material made for air pollution control able to sequestrate fine and ultrafine air particulate matter, *Sustain. Cities Soc.*, 2020, **53**, 101961, DOI: 10.1016/j.scs.2019.101961.

21 L. Benassi, R. Dalipi, V. Consigli, M. Pasquali, L. Borgese, L. E. Depero, *et al.*, Integrated management of ash from industrial and domestic combustion: a new sustainable approach for reducing greenhouse gas emissions from energy conversion, *Environ. Sci. Pollut. Res.*, 2017, **24**, 14834–14846, DOI: 10.1007/s11356-017-9037-y.

22 G. Sharma, M. Kaur, S. Punj and K. Singh, Biomass as a sustainable resource for value-added modern materials: a review, *Biofuels, Bioprod. Biorefin.*, 2020, **14**, 673–695, DOI: 10.1002/bbb.2079.

23 R. Prasad and M. Pandey, Rice husk ash as a renewable source for the production of value added silica gel and its application: An overview, *Bull. Chem. React. Eng. Catal.*, 2012, **7**, 1–25, DOI: 10.9767/bcrec.7.1.1216.1-25.

24 S. K. S. Hossain, L. Mathur and P. K. Roy, Rice husk/rice husk ash as an alternative source of silica in ceramics: A review, *J. Asian Ceram. Soc.*, 2018, **6**, 299–313, DOI: 10.1080/21870764.2018.1539210.

25 W. K. Setiawan, K.-Y. Chiang, *Crop Residues as Potential Sustainable Precursors for Developing Silica Materials: A Review*. Waste and Biomass Valorization, 2020. DOI: 10.1007/s12649-020-01126-x.

26 E. Bontempi, A. Zacco, L. Borgese, A. Gianoncelli, R. Ardesi and L. E. Depero, A new method for municipal solid waste incinerator (MSWI) fly ash inertization, based on colloidal silica, *J. Environ. Monit.*, 2010, **12**, 2093–2099, DOI: 10.1039/C0EM00168F.

27 A. Assi, F. Bilo, A. Zanoletti, J. Ponti, A. Valsesia, R. La Spina, L. E. Depero and E. Bontempi, Review of the reuse possibilities concerning ash residues from thermal process in a medium-sized urban system in Northern Italy, *Sustain*, 2020, **12**, 4193, DOI: 10.3390/su12104193.

28 L. Luyckx, G. H. J. de Leeuw and J. Van Caneghem, Characterization of Poultry Litter Ash in View of Its Valorization, *Waste Biomass Valorization*, 2020, **11**, 5333–5348, DOI: 10.1007/s12649-019-00750-6.

29 E. E. Codling, R. L. Chaney and J. Sherwell, Poultry Litter Ash as a Potential Phosphorus Source for Agricultural Crops, *J. Environ. Qual.*, 2002, **31**, 954–961, DOI: 10.2134/jeq2002.9540.

30 L. Hermann, T. Schaaf, Outotec manure, slurry, and sludge processing technology, in: *Phosphorus Recovery and Recycling*, Springer, 2019, app 403–417. DOI: 10.1007/978-981-10-8031-9_28.

31 *Welcome to BIOdat*. https://biodat.eu/pages/Home.aspx.

32 S. Andò, Gravimetric separation of heavy minerals in sediments and rocks, *Minerals*, 2020, **10**, 273, DOI: 10.3390/min10030273.

33 A. Assi, S. Federici, F. Bilo, A. Zacco, L. E. Depero and E. Bontempi, Increased sustainability of carbon dioxide mineral sequestration by a technology involving fly ash stabilization, *Materials*, 2019, **12**, 2714, DOI: 10.3390/ma12172714.

34 R. Klockenkämper and A. von Bohlen, *Total-Reflection X-Ray Fluorescence Analysis and Related Methods*. 2nd edn, Wiley, 2015.

35 L. Borgese, R. Dalipi, A. Riboldi, F. Bilo, A. Zacco, S. Federici, *et al.*, Comprehensive approach to the validation of the standard method for total reflection X-ray fluorescence analysis of water, *Talanta*, 2018, **181**, 165–171, DOI: 10.1016/j.talanta.2017.12.087.

36 Romanian Standard Association, *STAS 9621: 1982 Solid mineral fuels, Coke and semicoke, Determination of phosphorus content Part 3 Photocolorimetric method*, 1982.

37 A. Bosio, A. Gianoncelli, A. Zacco, L. Borgese, N. Rodella, D. Zanotti, *et al.*, A new nanotechnology of fly ash inertization based on the use of silica gel extracted from

rice husk ash and microwave treatment, *Proc. Inst. Mech. Eng., Part N*, 2014, **228**, 27–32, DOI: 10.1177/1740349913490683.

38 S. R. Kamath and A. Proctor, Silica gel from rice hull ash: Preparation and characterization, *Cereal Chem.*, 1998, **75**, 484–487, DOI: 10.1094/CCHEM.1998.75.4.484.

39 K. Sinkó, Influence of chemical conditions on the nanoporous structure of silicate aerogels, *Materials*, 2010, **3**, 704–740, DOI: 10.3390/ma3010704.

40 J. A. Santana Costa and C. M. Paranhos, Systematic evaluation of amorphous silica production from rice husk ashes, *J. Cleaner Prod.*, 2018, **192**, 688–697, DOI: 10.1016/j.jclepro.2018.05.028.

41 U. Kalapathy, A. Proctor and J. Shultz, A simple method for production of pure silica from rice hull ash, *Bioresour. Technol.*, 2000, **73**, 257–262, DOI: 10.1016/s0140-6701(01)80487-2.

42 B. Thongma and S. Chiarakorn, Recovery of silica and carbon black from rice husk ash disposed from a biomass power plant by precipitation method, *IOP Conf. Ser. Earth Environ. Sci.*, 2019, **373**, 012026, DOI: 10.1088/1755-1315/373/1/012026.

43 J. Alvarez, G. Lopez, M. Amutio, J. Bilbao and M. Olazar, Upgrading the rice husk char obtained by flash pyrolysis for the production of amorphous silica and high quality activated carbon, *Bioresour. Technol.*, 2014, **170**, 132–137, DOI: 10.1016/j.biortech.2014.07.073.

44 P. Terzioğlu, S. Yücel and Ç. Kuş, Review on a novel biosilica source for production of advanced silica-based materials: Wheat husk, *Asia-Pac. J. Chem. Eng.*, 2019, **14**, 2262, DOI: 10.1002/apj.2262.

45 J. A. Stammeier, B. Purgstaller, D. Hippler, V. Mavromatis and M. Dietzel, In-situ Raman spectroscopy of amorphous calcium phosphate to crystalline hydroxyapatite transformation, *MethodsX*, 2018, **5**, 1241–1250, DOI: 10.1016/j.mex.2018.09.015.

46 P. Staroń, Z. Kowalski, A. Staroń, J. Seidlerová and M. Banach, Residues from the thermal conversion of waste from the meat industry as a source of valuable macro- and micronutrients, *Waste Manag.*, 2016, **49**, 337–345, DOI: 10.1016/j.wasman.2016.01.018.

47 B. Valentim, D. Flores, A. Guedes, R. Guimarães, N. Shreya, B. Paul, *et al.*, Notes on the occurrence of phosphate mineral relics and spheres (phosphospheres) in coal and biomass fly ash, *Int. J. Coal Geol.*, 2016, **154–155**, 43–56, DOI: 10.1016/j.coal.2015.12.009.

48 J. Alvarez, G. Lopez, M. Amutio, J. Bilbao and M. Olazar, Physical Activation of Rice Husk Pyrolysis Char for the Production of High Surface Area Activated Carbons, *Ind. Eng. Chem. Res.*, 2015, **54**, 7241–7250.

49 L. Fang, Q. Wang, J. Li, C. S. Poon, C. R. Cheeseman, S. Donatello, *et al.*, Feasibility of wet-extraction of phosphorus from incinerated sewage sludge ash (ISSA) for phosphate fertilizer production: A critical review, *Crit. Rev. Environ. Sci. Technol.*, 2020, 1–33, DOI: 10.1080/10643389.2020.1740545.

50 L. Fang, J. Li, M. Z. Guo, C. R. Cheeseman, D. C. W. Tsang, S. Donatello, *et al.*, Phosphorus recovery and leaching of trace elements from incinerated sewage sludge ash (ISSA), *Chemosphere*, 2018, **193**, 278–287, DOI: 10.1016/j.chemosphere.2017.11.023.

51 S. Liang, H. Chen, X. Zeng, Z. Li, W. Yu, K. Xiao, *et al.*, A comparison between sulfuric acid and oxalic acid leaching with subsequent purification and precipitation for phosphorus recovery from sewage sludge incineration ash, *Water Res.*, 2019, **159**, 242–251, DOI: 10.1016/j.watres.2019.05.022.

52 K.-J. Hong, N. Tarutani, Y. Shinya and T. Kajiuchi, Study on the recovery of phosphorus from waste-activated sludge incinerator ash, *J. Environ. Sci. Health, Part A: Toxic/Hazard. Subst. Environ. Eng.*, 2005, **40**, 617–631, DOI: 10.1081/ESE-200046614.

53 K. I. Biswas, H. Harada, K. Ohto and H. Kawakita, Leaching of phosphorus from incinerated sewage sludge ash by means of acid extraction followed by adsorption on orange waste gel, *J. Environ. Sci.*, 2009, **21**, 1753–1760, DOI: 10.1016/S1001-0742(08)62484-5.

54 H. Xu, P. He, W. Gu, G. Wang and L. Shao, Recovery of phosphorus as struvite from sewage sludge ash, *J. Environ. Sci.*, 2012, **24**, 1533–1538, DOI: 10.1016/S1001-0742(11)60969-8.

55 S. Petzet, B. Peplinski and P. Cornel, On wet chemical phosphorus recovery from sewage sludge ash by acidic or alkaline leaching and an optimized combination of both, *Water Res.*, 2012, **46**, 3769–3780, DOI: 10.1016/j.watres.2012.03.068.

56 N. Semerci, S. Ahadi and S. Coşgun, Comparison of dried sludge and sludge ash for phosphorus recovery with acidic and alkaline leaching, *Water Environ. J.*, 2020, **0**, 1–12, DOI: 10.1111/wej.12633.

57 A. Fahimi, S. Federici, L. E. Depero, B. Valentim, I. Vassura, F. Ceruti, L. Cutaia and E. Bontempi, Evaluation of the sustainability of technologies to recover phosphorus from sewage sludge ash based on embodied energy and CO2 footprint, *J. Cleaner Prod.*, 2021, **289**, 125762, DOI: 10.1016/j.jclepro.2020.125762.

58 M. Smol, J. Kulczycka, A. Henclik, K. Gorazda, B. Tarko and Z. Wzorek, *Sewage Sludge Ash (SSA) as a Phosphate Fertilizer in the Aspect of Legal Regulations*, 2015, pp. 323–328. DOI: 10.1201/b18853-54.

59 H. Kominko, K. Gorazda, Z. Wzorek and K. Wojtas, Sustainable Management of Sewage Sludge for the Production of Organo-Mineral Fertilizers, *Waste Biomass Valorization*, 2018, **9**, 1817–1826, DOI: 10.1007/s12649-017-9942-9.

60 Regulation (E. C) *No 2003/2003 of the European Parliament and of the Council relating to fertilizers*, 2003.

61 Regulation (E. U) *2019/1009 of the European Paliament and of the Council laying down rules on the making available on the market of EU fertilising products*, 2019.

62 X. Meng, X. Liu, Q. Huang, H. Gao, K. Tay and J. Yan, Recovery of phosphate as struvite from low-temperature combustion sewage sludge ash (LTCA) by cation exchange, *Waste Manag.*, 2019, **90**, 84–93, DOI: 10.1016/j.wasman.2019.04.045.

63 L. Fang, J. Li, S. Donatello, C. R. Cheeseman, Q. Wang, C. S. Poon, *et al.*, Recovery of phosphorus from incinerated sewage sludge ash by combined two-step extraction and selective precipitation, *Chem. Eng. J.*, 2018, **348**, 74–83, DOI: 10.1016/j.cej.2018.04.201.

64 Q. Wang, J. Li, P. Tang, L. Fang and C. S. Poon, Sustainable reclamation of phosphorus from incinerated sewage sludge ash as value-added struvite by chemical extraction, purification and crystallization, *J. Cleaner Prod.*, 2018, **181**, 717–725, DOI: 10.1016/j.jclepro.2018.01.254.

65 M. M. Thant Zin and D. J. Kim, Struvite production from food processing wastewater and incinerated sewage sludge ash as an alternative N and P source: Optimization of multiple resources recovery by response surface methodology, *Process Saf. Environ. Prot.*, 2019, **126**, 242–249, DOI: 10.1016/j.psep.2019.04.018.

66 I. Rech, M. Y. Kamogawa, D. L. Jones and P. S. Pavinato, Synthesis and characterization of struvite derived from poultry manure as a mineral fertilizer, *J. Environ. Manage.*, 2020, **272**, 111072, DOI: 10.1016/j.jenvman.2020.111072.

67 L. Luyckx, S. Geerts and J. Van Caneghem, Closing the phosphorus cycle: Multi-criteria techno-economic optimization of phosphorus extraction from wastewater treatment sludge ash, *Sci. Total Environ.*, 2020, **713**, 135543, DOI: 10.1016/j.scitotenv.2019.135543.

68 Y. Liu and H. Qu, Design and optimization of a reactive crystallization process for high purity phosphorus recovery from sewage sludge ash, *J. Environ. Chem. Eng.*, 2016, **4**, 2155–2162, DOI: 10.1016/j.jece.2016.03.042.

69 J. Li, Z. Chen, Q. Wang, L. Fang, Q. Xue, C. R. Cheeseman, *et al.*, Change in re-use value of incinerated sewage sludge ash due to chemical extraction of phosphorus, *Waste Manag.*, 2018, **74**, 404–412, DOI: 10.1016/j.wasman.2018.01.007.

70 S. Donatello, Characteristics of incinerated sewage sludge ashes: Potential for phosphate extraction and re-use as a pozzolanic material in construction products, PhD thesis, Imperial College London, 2009. , DOI: 10.13140/RG.2.2.33926.63040.